ORIGINAL ARTICLE

A C G publications

Org. Commun. 8:3 (2015) 78-89

organic communications

Phthalimide containing donor-acceptor polymers for effective dispersion of single-walled carbon nanotubes

Baris Yilmaz [1], Josiah Bjorgaard[1], Zhenghuan Lin[1] and Muhammet E. Köse[*2]

[1] *Department of Chemistry and Biochemistry, North Dakota State University, Fargo, North Dakota, 58108, USA*

[2] *TUBITAK Marmara Research Center, Gebze, Kocaeli, 41470 Türkiye*

(Received April 7, 2015; Revised July 15, 2015; Accepted July 20, 2015)

Abstract: Single-walled carbon nanotubes have been dispersed by novel phthalimide containing donor-acceptor type copolymers in organic media. Brominated phthalimide comonomer has been copolymerized with several electron rich structures using Suzuki and Stille coupling reactions. Carbon nanotube dispersion capability of the resultant polymers has been assessed by exploiting the non-covalent interaction of nanotube surface with the π-system of conjugated backbone of polymers. Four polymers have been found to be good candidates for individually dispersing nanotubes in solution. In order to identify the dispersed nanotube species, 2D excitation-emission map and Raman spectroscopy have been performed. Molecular dynamics modelling has been utilized to reveal the binding energies of dispersants with the nanotube surface and the simulation results have been compared with the experimental findings. Both experimental and theoretical results imply the presence of a complex mechanism that governs the extent of dispersion capacity and selectivity of each conjugated polymeric dispersant in solubilizing carbon nanotubes.

Keywords: Phthalimide polymers, carbon nanotubes, separation, Raman spectroscopy, molecular dynamics simulations.

1. Introduction

Single-walled carbon nanotubes (SWNTs) can be exploited in applications such as optoelectronics, fibers, and nanocomposites. Most of the relevant applications require individually sorted carbon nanotubes samples with known chiralities. However, almost all of the synthesis methods of SWNTs yield to nanotubes with many different chiralities, which have been indexed as (n,m). It is well known that some of these chiral tubes are semiconducting whereas the others display metallic properties. In addition, due to variation in (n,m) index, the nanotubes possess various diameters and such variation is reflected upon their mechanical properties. Thus, in order to exploit SWNTs in applications or in fundamental research, chirality specific sorting of nanotubes is essential. Therefore, many research groups worldwide focus on strategies to develop an experimental method to individually sort carbon nanotubes in bulk scale. It is important to note that the sp^2 hybridized carbon atom structure of SWNTs should be preserved during dispersion experiments in order to keep the electronic properties of nanotubes unaltered. The obvious strategy is then use of specific dispersant molecules that can interact with nanotube surface

[*] Corresponding Author: E-mail: erkan.kose@tubitak.gov.tr

The article was published by Academy of Chemistry of Globe Publications
www.acgpubs.org/OC/index.htm © Published 08/10/2015 EISSN:1307-6175

with van der Waals interactions or π-π interactions. Conjugated materials with aromatic π-system present themselves as ideal materials that can be used for this purpose.

Indeed, selective dispersions of carbon nanotubes can be obtained via non-covalent interactions in the presence of polyaromatic hydrocarbons,[1, 2] conjugated polymers,[3] or nanotweezers.[4] Conjugated polymers have gained considerable attention in recent years as a structural motif to disperse SWNTs. The mechanism of the dispersion is believed to be strong π-π interaction between nanotube surface and π-system on conjugated polymer as well as helical wrapping of polymer chain around the tubes.[5, 6] Conjugated polymers as dispersants can debundle SWNTs in high concentrations. Furthermore, the repeat unit structure of the polymer can be tailored to function for a particular purpose.[7] Mostly, polyfluorenes,[8-11] poly(phenylenevinylenes),[12, 13] poly(phenyleneethinylenes),[14, 15] polycarbazoles,[16] and polythiophenes[17] have been used as dispersing polymers. In some cases, specific dispersion of some type of carbon nanotubes has been achieved with such polymers. Specifically, polyfluorenes display strong selectivity toward semiconducting SWNTs with large chiral angles ($20° \leq \theta \leq 30°$).[9-11] Poly(9,9-dioctlyfluorene-2,7-diyl) almost exclusively disperses semiconducting SWNTs. Field-effect transistors made with such selectively dispersed nanotubes confirmed the chiralities measured with optical spectroscopy techniques.[18] Copolymers of 9,9-dialkylfluorenes with phenylene-1,4-diyl,[10] thiophene-2,5-diyl,[19] 2,2'-bithiophene-5,5'-diyl,[11] benzo-2,1,3-thiadiazole-4,7-diyl,[8] and anthracene-9,10-diyl[11] were also found to be effective in dispersing SWNTs. For instance, the copolymer with benzo-2,1,3-thiadiazole-4,7-diyl and 9,9-dioctylfluorenes has displayed strong selectivity towards (10,5) and (11,4) nanotubes in toluene.[11] The same polymer, however, exhibited much less selectivity in another organic solvent (tetrahydrofuran (THF)).[10]

In this work, we study the carbon nanotube dispersion capability of novel six phthalimide containing donor-acceptor type copolymers. To our knowledge, phthalimide bearing conjugated polymers have never been used in SWNT dispersion studies. Thus, we aimed to examine the effect of phthalimide group on dispersion capacity as well as understand structure-property relationships that can be used to maximize solubility of SWNTs in organic solvents as individual tubes. It is also our goal to reveal how conjugated backbone structural variation affects the selectivity of dispersion for some nanotubes with specific chirality.

2. Results and discussion

The structures and synthesis scheme of novel polymers used in this work are given in Scheme 1. The corresponding comonomers were synthesized by using the known literature methods as mentioned in Experimental section. PPC, PPCO, and PPCA were synthesized using Suzuki coupling reaction whereas PPTO, PPTA, and PPCT were synthesized by Stille coupling method. The molecular weights of polymers are listed in Table 1 along with the optical band gap and the electrochemical data. The polymerization yield was in general low (30-50%), which reflects itself upon on low molecular weights measured with gel-permeation chromatography. PPCT had the highest molecular weight among the polymers synthesized in this work. However, the molecular weight had little impact on dispersion capability of polymers as will be supported by the simulation efforts and experimental findings below.

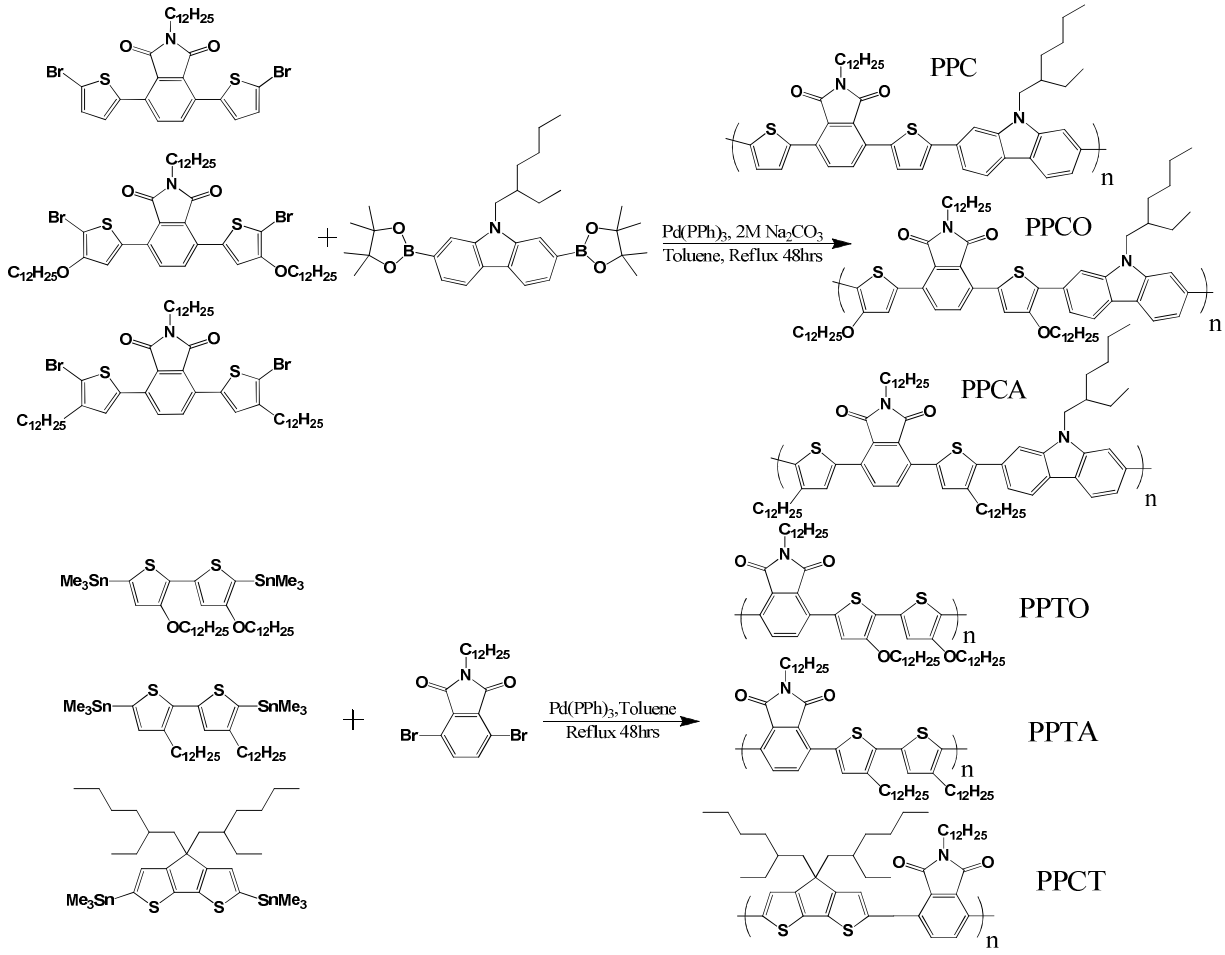

Figure 1. The synthesis scheme of conjugated polymers with Suzuki and Stille coupling reactions

The optical band gap of synthesized polymers varied from 2.03 eV to 2.55 eV. The spectral profiles of the polymers in solution can be found in Figure 2 (left). The cyclic voltammograms of the polymers for oxidation scan were given Figure S1 and the measured HOMO levels were given in Table 1. LUMO levels were estimated by summing up HOMO energies with solution band gaps of the corresponding conjugated polymers. The addition dodecyloxy groups on thiophene units raised the HOMO level of PPC (-5.61 eV) to -5.18 eV (PPCO). The LUMO level remained unchanged between PPC and PPCO. Thus, the band gap reduction was mainly achieved by introduction of electron-rich alkoxy group on conjugated backbone, which in turn the decreased the band gap of PPCO to the lowest magnitude among these polymers. However, the HOMO level energy of PPCA was similar to that of PPC when dodecyl group was introduced on thiophene groups. Since there is little electron-donating ability of alkyl groups on conjugated chain, the frontier energy levels and optical band gap of PPC and PPCA turned out to be very similar to each other.

The electronic effect of dodecyloxy and dodecyl groups can also be observed by comparing the electrochemical and spectroscopic data in between PPTA and PPTO polymers. Again, the introduction of dodecyloxy electron-rich group on bithiophene units caused an increase in the HOMO level. Interestingly, the LUMO level of PPTO was also affected by the presence of alkoxy group, which in turn led to 0.28 eV band gap reduction when going from PPTA to PPTO. Fused bithiophene linkage (cyclopentadithiophene)

was used in PPCT and its effect on electronic properties should be compared to those of PPTA. PPCT displayed deeper HOMO and LUMO levels than those of PPTA and thus has lower band gap (2.11 eV) than that of PPTA. This implies that the fused comonomers were better in terms of reducing the band gap in conjugated systems.

Table 1. Weight-averaged molecular weight (M_w), number-averaged molecular weight (M_n), polydispersity index (PDI), solution optical band gap, and frontier energy levels of synthesized polymers.

Polymer	M_w (kDa)	M_n (kDa)	PDI	E_g^{soln} (eV)	HOMO (eV)	LUMO (eV)
PPC	6.5	3.6	1.8	2.47	-5.61	-3.14
PPCA	4.5	2.1	2.1	2.55	-5.58	-3.03
PPCO	4.0	3.4	1.2	2.03	-5.18	-3.15
PPTA	3.8	2.3	1.7	2.40	-5.33	-2.93
PPTO	6.0	4.3	1.4	2.12	-5.23	-3.11
PPCT	20.4	15.1	1.4	2.11	-5.42	-3.31

Carbon nanotubes were dispersed in tetrahydrofuran solvent with the aid of the polymers given in Scheme 1. Both PPC and PPCT did not produce stable suspensions for further analysis. The remaining four polymers, however, have been found to individually solubilize SWNTs quite well. The optical absorbance data collected (Figure 2, right) at visible and near-infrared region helped us to identify the chiralities of the nanotubes dispersed by these polymers. Since the same experimental methodology is followed for each polymer dispersant, it is safe to claim that PPTO worked as the best dispersing agent among the polymers studied here. However, there was no selectivity towards specific nanotubes. It looked like all of the polymers disperse similar nanotubes but to a different extent, as can be seen from the variation in optical density. The fact that we could clearly differentiate all the peaks in the spectra pointed out the individual nature of the tubes dispersed; that is the nanotubes were not in bundled state when wrapped with polymer chains. Some of the identified tubes have chiral indices such as (6,5), (9,4), (7,5), and (7,3), which were mostly observed and abundant in carbon nanotube samples prepared by high pressure carbon monoxide (HiPCO) process.

In order to further prove that the nanotubes were individually dispersed by polymers, 2-dimensional (2D) excitation-emission plot has been generated for each polymer-SWNT hybrid solution (Figure 3). The chiral indices of the tubes have been identified from the emission maxima on these 2D maps. The previously distinguished (9,4), (7,5), and (7,6) nanotubes from optical spectra were also observed in the photoluminescence map. In addition, major nanotube species such as (8,4), (11,1), (9,3), and (8,3) were found to exist in all polymer-SWNT hybrids. Intensities of emission maxima for some nanotube species varied from one polymer dispersant to other. That is, there were some differences in which the extent of dispersion for a particular nanotube varies among the dispersant polymers. Yet, it was clear that similar nanotubes and nanotube families are solubilized in THF solution. Figure 2 also presents a transmission of electron microscope (TEM) image of PPTO-SWNT hybrid on copper substrate. Most of the nanotubes in the TEM image were individual nanotubes, in agreement with the spectroscopic observations. More TEM images are provided in Figure S2.

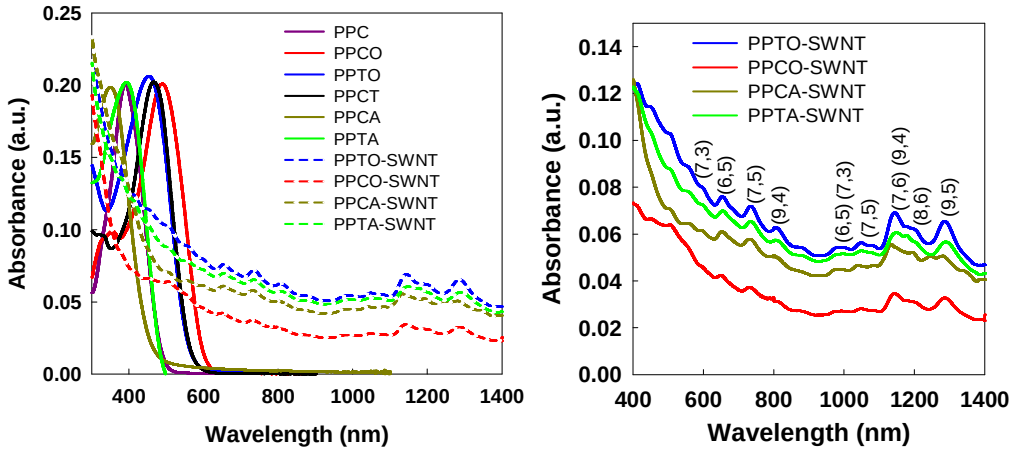

Figure 2. Optical absorbance spectra of polymers and polymer-SWNT complexes in THF solution are given in the left panel. The same spectral data with identified nanotube species are illustrated at the right panel

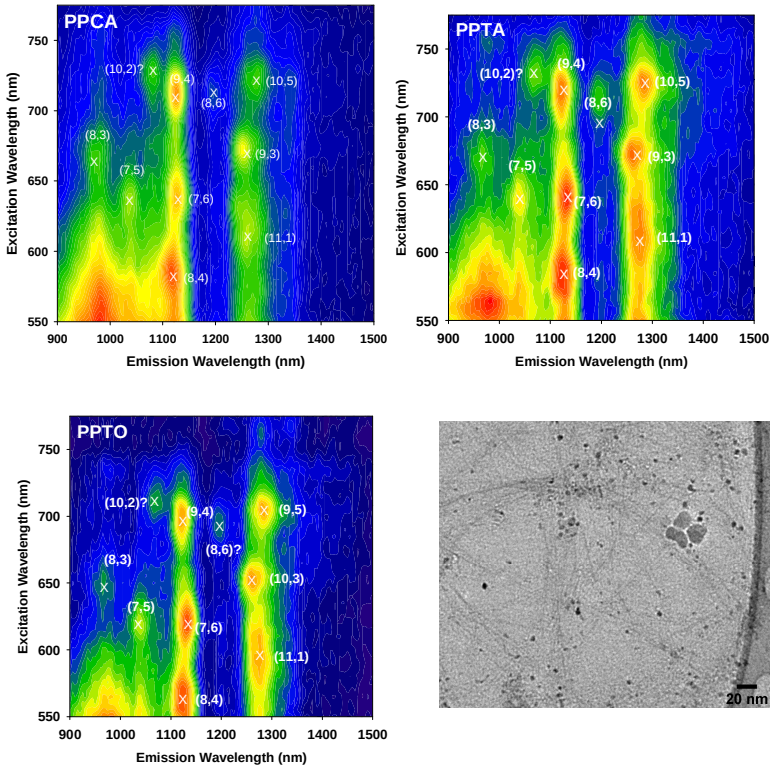

Figure 3. 2D excitation-emission maps of polymer-SWNT solutions. Transmission electron microscope image of PPTO-SWNT hybrids on cupper surface is given lower right panel

Although both UV spectroscopy and photoluminescence spectroscopy are useful in detecting the chirality of nanotube samples dispersed with a specific agent, those spectroscopic techniques give little information whether the metallic nanotubes present in the solubilized sample. Metallic nanotubes do not

have photoluminescence signature and it is hard to observe them with UV analysis unless the solution contains purely metallic species. Raman spectroscopy, on the other hand, can give an idea how effective an agent is in dispersing carbon nanotubes, specifically the metallic fraction. One can work on solid samples using Raman spectroscopy, thus the collected results with novel dispersants can be compared with those of pristine samples for a detailed assessment of selective solubilization process.

Sodium dodecyl sulfate (SDS) is the most common dispersant to study individualized carbon nanotubes in solution. The radial-breathing mode (RBM) frequencies were collected between 120 and 320 cm^{-1}. At 532 nm excitation, the peaks that correspond to semiconducting nanotubes appear between 220 and 300 cm^{-1} and for metallic nanotubes the range is between 180 and 230 cm^{-1}. Figure 3 (top left panel) shows that the SDS sample had negligible Raman resonance peak at the metallic range whereas polymer dispersants displayed distinct Raman peaks at the same region. Furthermore, the relative intensity of G^- band (~1525 cm^{-1}) to G^+ band (~1580 cm^{-1}) at 532 nm excitation is a useful indicator for the metallic nanotube enrichment in the studied samples. The broadening of G^- band with the metallic content was another strong indicator for the presence of metallic nanotubes (Figure 4, top right panel). In this regard, all of the polymeric dispersants showed higher inclination to disperse metallic nanotubes than SDS surfactant except PPTO.

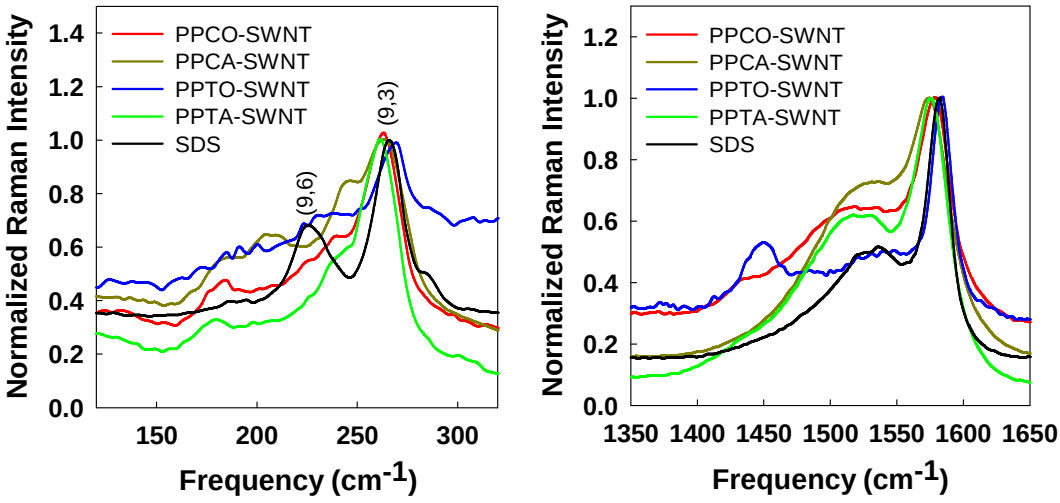

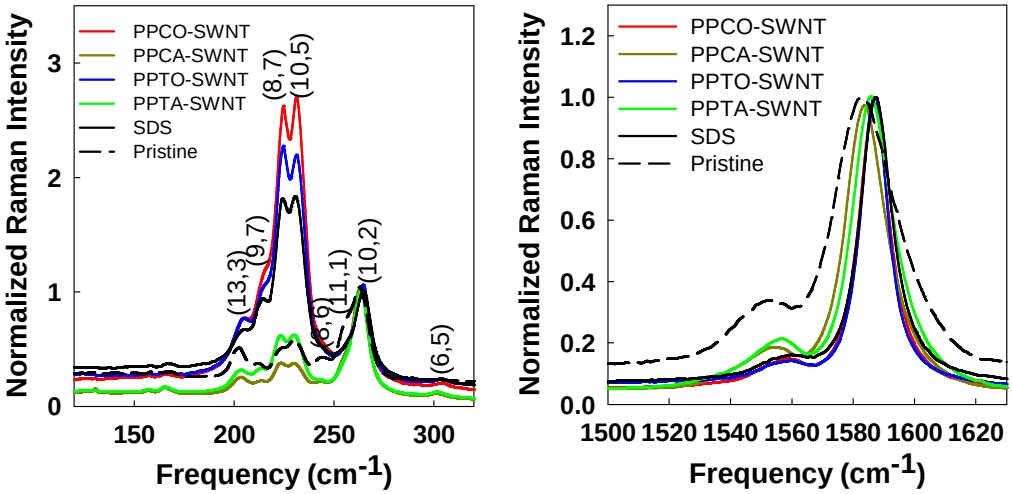

Figure 4. Normalized Raman spectra of polymer-SWNT hybrids recorded on dried samples. The upper two panels were obtained with excitation at 532 nm whereas lower panels were recorded with 785 nm excitation laser line.

The Raman spectra were also collected with excitation at 785 nm and the aforementioned laser line is mostly in resonant with semiconducting nanotubes. At RBM region (Figure 4, bottom left panel), the pristine sample displayed similar peaks with those of SDS sample but with varying intensities for each nanotube type. (8,7) and (10,5) nanotubes were more pronounced in SDS sample, showing the tendency of SDS surfactant to solubilize those nanotube species. PPTO and PPCO also favored dispersing (8,7) and (10,5) nanotubes in comparison to (10,2) species. The RBM profile of PPTA and PPCA samples mostly resembled that of pristine sample. The G^-/G^+ band intensity ratios of PPTA- and PPCA-SWNT hybrids were higher than that of SDS sample (Figure 4, bottom left panel), in agreement with the conclusions drawn from the analysis of data collected at 532 nm. It is interesting to see that although some of the polymer dispersants disperse metallic nanotubes better than SDS surfactant; the metallic/semiconducting ratio in pristine sample was still higher. That means, the polymeric dispersants still behaved as better agents in solubilizing semiconducting tubes than metallic ones.

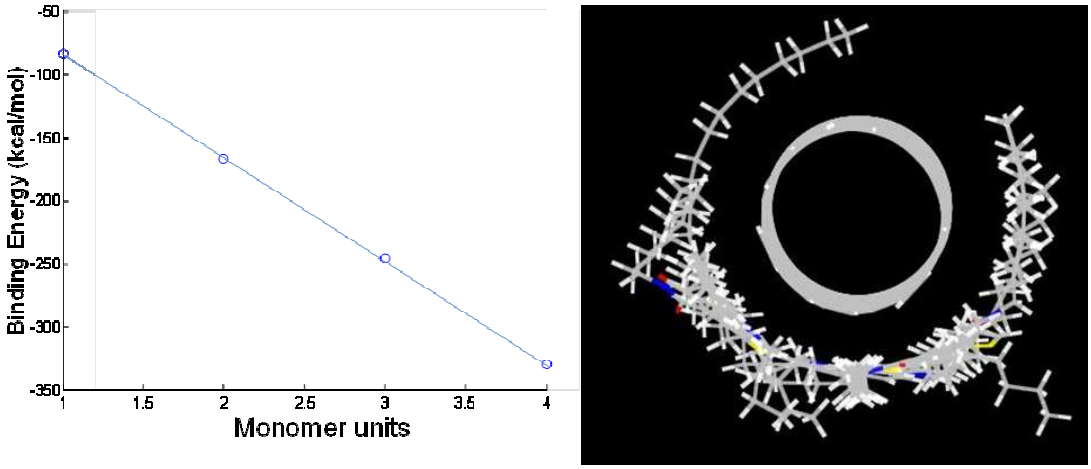

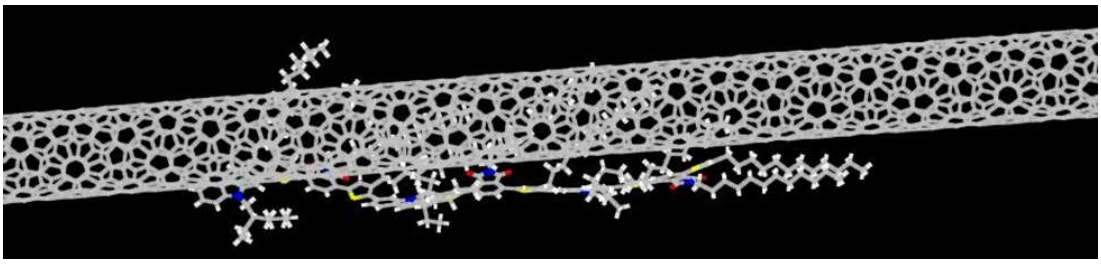

Figure 5. The variation in the binding energy of PPTA oligomers with increasing repeat unit size is given in top left corner. The wrapping geometry is illustrated from two snapshots of molecular dynamics simulation of PPTA trimer on (9,4) nanotube.

In order to further understand how conjugated polymers interact with carbon nanotube surface, molecular dynamics simulations were performed with MM3 force field. The relevant methodological details can be found in the Experimental section below. To examine the effect of oligomer length on the binding energy, energy minimized structures were determined for oligomers of PPTA model polymer consisting of 1-4 repeat units. The initial configurations for these simulations consisted of polymers approximately wrapped around the CNTs with alkyl chains pointing in opposite directions. The energy minimized structures are well wrapped. That is, each unit of the oligomeric backbone was in nearly the same proximity to the CNT surface. The binding energy calculated from these energy minimized structures was quantitatively linear with the number of repeat units (Figure 5). There was no nonlinear change in intermolecular effects on the binding energy upon increasing the oligomer length in these simulations. This finding is significant as one only needs to perform theoretical calculation on one repeat unit and if molecular weight or size of the oligomer is known, then it is straightforward to calculate the total binding energy of the dispersant in question. Since we know the number average molecular weight of each dispersant polymers used in this study, we can now predict the total binding energy for each polymer and theoretically rank the binding energies and hence the dispersion power.

PPCA and PPCO repeat units had a binding energy of ~78 kcal/mole whereas PPTO and PPTA had a binding energy of ~60 kcal/mole (Figure 6). The simulations predicted whether one uses dodecyl or dodecyloxy group, the binding energies do not change within the error of simulation. Simulations also predicted the size of the solubilizing group on polymer backbone is very important since almost half of the binding energy comes from contributions from solubilizing groups. Nonetheless, these simulations are performed in the gas phase and the effect of alkyl or alkoxy groups in solubilizing the nanotubes could be much less in solvated medium. By taking account the number of repeat units at each system, we found that (9,4) nanotube should be solubilized most in the following order; PPCO > PPTO > PPCA > PPTA. However, experimental results suggest that PPTO disperses best followed by PPTA, PPCA, and then PPCO. The apparent mismatch between the simulated results and the experimental findings could be explained by the following reasons; (1) the lack of introduction solvent molecules (THF) into simulation box, (2) the lack of appropriate parameters in MM3 code for accurately accounting dispersion interactions, (3) the lack of simulated data with other types of nanotubes due to limitations in computational power and time, and (4) possible errors in determining accurate M_n due to relatively low magnitude of the measured data (error margin is high).

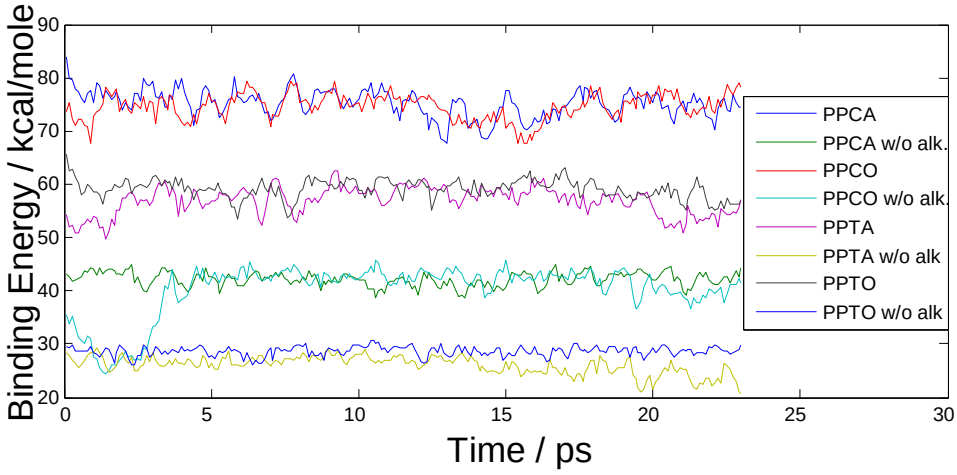

Figure 6. Molecular dynamics simulation of binding energies for each repeat unit of polymer with dodecyl or dodecyloxy chains and also with truncated methyl or methoxy analogues

3. Experimental

3.1. Materials and apparatus: All the chemicals were purchased from Sigma Aldrich and used as received. The reactions that were air sensitive were performed in glove box in a nitrogen atmosphere unless otherwise stated. Freshly distilled THF from sodium with benzophenone as indicator was used. Gas chromatography-mass spectrometry was obtained on an Agilent Technologies 7890A GC system. ^{1}H NMR and ^{13}C NMR spectra were recorded on a Varian 400 MHz and 500 MHz NMR instruments. The solvents for various NMR experiments are mentioned in the text. The chemical shifts were reported in parts per million (ppm) relative to internal standard TMS (0 ppm). All UV-Vis spectra were recorded using a Varian Cary 50 and Cary 5000 spectrometer. Photoluminescence spectra were taken on a Jobin-Yvon Fluorolog 3 fluorescence spectrometer, which utilizes a liquid nitrogen cooled near-IR InGaAs detector. The molecular weights were measured using Gel Permeation Chromatography (GPC) with THF as an eluent, with a flow rate of 1 mL/min on a Waters Modular system with 2410 Refractive Index detector and 515 pump. The system utilized a styragel 4E and 5E column and calibrated with polystyrene standards. Transmission electron microscopy image was collected with JEOL JEM-100 CX II system. Cyclic voltammetry experiments were carried out on an EDAQ Potentiostat 466 system. The three-electrode setup consists of a Pt working electrode, a Pt-wire counter electrode, and an Ag/AgCl reference electrode. $[Bu_4N]PF_6$ (0.1 M, CH_3CN) was used as a supporting electrolyte.

3.2. Synthesis of Monomers; 4,7-bis(5-bromothiophen-2-yl)-2-dodecylisoindoline-1,3-dione,[20] 9-(2-ethylhexyl)-2,7-bis(4,4,5,5- tetramethyl-1,3,2-dioxaborolan-2-yl)-9H-carbazole,[21] (4,4-bis(2-ethylhexyl)-4H-cyclopenta[1,2-b:5,4-b']dithiophene-2,6-diyl)bis(trimethylstannane),[22] 4,7-dibromo-2-dodecylisoindoline-1,3-dione,[20] (3,4'-didodecyl-[2,2'-bithiophene]-5,5'-diyl) bis(trimethylstannane) [US Patent WO 2010/079064 A2], (3,4'-bis(dodecyloxy)-[2,2'-bithiophene]-5,5'-diyl) bis(trimethylstannane)6,4-(5-bromo-3-dodecylthiophen-2-yl)-7-(5-bromo-4-dodecylthiophen-2-yl)-2-dodecylisoindoline-1,3-dione [US Patent US 2010/0252112], 4-(5-bromo-3-(dodecyloxy)thiophen-2-yl)-7-(5-bromo-4-(dodecyloxy)thiophen-2-yl)-2-dodecyl isoindoline -1,3-dione[US Patent 2013/0035464A1] were synthesized according to cited literature.

3.3. Synthesis of Polymers; For Suzuki-Murayama coupling, dibromo compound (0.5 mmol) and boronic ester compound (0.5 mmol) were placed in double neck 100-mL round bottom flask along with 20 mL of toluene and 20 ml of 2 M Na_2CO_3 solution. The system was purged with nitrogen gas for 30 minutes before placing the $Pd(PPh_3)_4$ catalyst. Reaction mixture was, then, refluxed for 48 hrs. At the end of reaction, the reaction mixture was poured drop wise into 150 mL methanol. The suspension was stirred for one hour and then filtered through a Soxhlet thimble. The thimble was placed into a Soxhlet apparatus and the solid was washed with methanol, acetone, hexanes, and chloroform, respectively. Chloroform fraction is, then, used for polymer extraction. A similar experimental protocol was followed for Stille coupling reactions. In Stille coupling experiments, dibromo compound and tin coupled compound were placed in double neck 100-mL round bottom flask with 20 mL anhydrous toluene. The system was purged with nitrogen gas for 30 minutes before placing the $Pd(PPh_3)_4$ catalyst. The reaction mixture was heated to reflux condition and kept at that temperature for 48 hrs. The rest of the procedure is the same as Suzuki coupling reaction.

(*PPC*); ^{1}H NMR ($CDCl_3$, 400 MHz): 8.09 (br, 2H), 7.95 (br, 4H), 7.57-7.35 (br, 4H), 7.27 (br, 2H), 4,29 (br, 4H), 4,17 (br,2H) 3.71 (br, 2H), 2.10 (br,2H), 1.19-1.68(br, 28H), 0.74-0.95 (br, 12H)
(*PPCA*); ^{1}H NMR ($CDCl_3$, 400 MHz): 8.10 (br, 2H), 7.87 (br, 4H), 7.55 (br, 2H), 7.47 (br, 2H), 3.72 (br, 4H), 3.275 (br,3H),1.6-1.8 (br, 6H), 1.19-1.5(br, 62H), 0.74-0.95 (br, 12H)
(*PPCO*); ^{1}H NMR ($CDCl_3$, 400 MHz): 8.09 (br, 2H), 7.85 (br, 2H), 7.57 (br, 2H), 7.27 (br, 2H), 4,29 (br, 4H), 4,14 (br,2H) 3.72 (br, 2H), 2.10 (br,4H), 1.19-1.68(br, 32H), 0.74-0.95 (br, 15H)
(*PPTA*); ^{1}H NMR ($CDCl_3$, 400 MHz): 8.05 (br, 2H), 7.87 (br, 2H), 3.67 (br, 2H), 2.75 (br,4H),1.6-1.8 (br, 6H), 1.19-1.5(br, 54H), 0.74-0.95 (br, 9H)
(*PPTO*); ^{1}H NMR ($CDCl_3$, 400 MHz): 8.05 (br, 2H), 7.87 (br, 2H), 4.27 (br, 4H), 3.75 (br,2H),1.6-1.8 (br, 6H), 1.19-1.5(br, 54H), 0.74-0.95 (br, 9H)
(*PPCT*); ^{1}H NMR ($CDCl_3$, 400 MHz): 8.10 (br, 2H), 6.67 (s, 2H), 3.76 (br, 4H), 2.10 (br,4H), 1.19-1.68(br, 22H), 0.74-0.95 (br, 14H)

3.4. SWNT-Polymer Dispersions; In a typical experiment, 5 mg of SWNT sample (HiPco, Unidym, Inc., Lot#P2150) was added to a solution of polymer in THF (45 mg/15 mL). The mixture was ultrasonicated for 15 min by using Omni Raptor 450 Homogenizer (tip sonication, 20% power), followed by a bath sonication for 3 hrs. The resulting solution was centrifuged for 15 min at 5500 rpm (Beckman SW 40Ti Swing bucket). The supernatant was carefully transferred by pipette to a vial, producing dark colored and stable nanotube-polymer dispersion. The isolated supernatant was filtered through a 200 nm pore diameter Teflon membrane, and repeatedly washed with THF until the filtrate was colorless to ensure the removal of all excess free polymers. Then, 6 mL of THF was added to the recovered SWNT residue, and the solution was further sonicated for 15 min. The resulting dark suspension remained stable for at least 2 months without any observable precipitation.
3.5. Theoretical Methods; The non-covalent binding of oligomers on carbon nanotubes was modeled using (9,4) nanotubes and monomers/oligomers of relevant compounds. These simulations were carried out using the TINKER package.[23] A modified version of the MM3 forcefield was constructed to accommodate molecules in this study by copying native parameters from structures with similar geometry. Binding energy was calculated according to equation

$$V_B = E_{NT-D} - (E_{NT} + E_D) \quad (1)$$

where V_B is the binding energy, $E_{NT\text{-}D}$ is the total energy of the bound SWNT/dispersant complex, and E_{NT} and E_D are the total energy calculated for isolated SWNT and dispersant in the same nuclear configuration as in the complexed molecules. In the MM3 forcefield, the nonbonded energy term is the result of two pairwise contributions, electrostatic and van der Waals interactions. The electrostatic interaction is calculated from Coulomb's law, while the van der Waals interaction is calculated according the Lennard-Jones potential.

Minimized energy structures were determined for single repeat units of PPCA, PPCO, PPTA, and PPTO structures and structures with alkyl chains truncated to methyl or methoxy groups. These minimum energy structures were used as initial configurations for molecular dynamics simulations. Molecular dynamics were carried out using the modified Beeman integration scheme implemented in the TINKER package with constant temperature thermostat at 300K and time step of 0.1 fs. The binding energy was calculated at each time step (Figure 6).

4. Conclusion

In conclusion, we have synthesized six novel phthalimide containing polymers and used them as dispersants to individually solubilize single walled carbon nanotubes in solution. PPTA, PPTO, PPCA, and PPCO polymers were found to be effective in dispersing nanotubes. PPTA and PPCA showed greater tendency to disperse metallic nanotubes than the other polymers. Theoretical simulations were in partial agreement with the experimental observations. It is clear that the solubilization mechanism of dispersants is very complex and it requires high level theory and more thorough analysis to better judge the undergoing phenomena. Combined, phthalimide containing conjugated copolymers can be used to disperse carbon nanotubes as long as right structure is chosen for the intended study.

Acknowledgements

This work was supported by NSF Grant #EPS-0814442, DOE under award #DE-FG52-08NA28921, and TUBITAK BIDEB Fellowship Program.

References

[1] Voggu, R.; Rao, K. V.; George, S. J.; Rao, C. N. R., A Simple Method of Separating Metallic and Semiconducting Single-Walled Carbon Nanotubes Based on Molecular Charge Transfer. *Journal of the American Chemical Society* **2010,** *132*, 5560-5561.

[2] Yilmaz, B.; Bjorgaard, J.; Colbert, C. L.; Siegel, J. S.; Kose, M. E., Effective Solubilization of Single-Walled Carbon Nanotubes in THF Using PEGylated Corannulene Dispersant. *Acs Applied Materials & Interfaces* **2013,** *5*, 3500-3503.

[3] Zhao, Y.-L.; Stoddart, J. F., Noncovalent Functionalization of Single-Walled Carbon Nanotubes. *Accounts of Chemical Research* **2009,** *42*, 1161-1171.

[4] Wang, F.; Matsuda, K.; Rahman, A. F. M. M.; Peng, X.; Kimura, T.; Komatsu, N., Simultaneous Discrimination of Handedness and Diameter of Single-Walled Carbon Nanotubes (SWNTs) with Chiral Diporphyrin Nanotweezers Leading to Enrichment of a Single Enantiomer of (6,5)-SWNTs. *Journal of the American Chemical Society* **2010,** *132*, 10876-10881.

[5] Yi, W.; Malkovskiy, A.; Chu, Q.; Sokolov, A. P.; Colon, M. L.; Meador, M.; Pang, Y., Wrapping of Single-Walled Carbon Nanotubes by a π-Conjugated Polymer: The Role of Polymer Conformation-Controlled Size Selectivity. *The Journal of Physical Chemistry B* **2008,** *112*, 12263-12269.

[6] Kang, Y. K.; Lee, O.-S.; Deria, P.; Kim, S. H.; Park, T.-H.; Bonnell, D. A.; Saven, J. G.; Therien, M. J., Helical Wrapping of Single-Walled Carbon Nanotubes by Water Soluble Poly(p-phenyleneethynylene). *Nano Letters* **2009,** *9*, 1414-1418.

[7] Berton, N.; Lemasson, F.; Tittmann, J.; Stürzl, N.; Hennrich, F.; Kappes, M. M.; Mayor, M., Copolymer-Controlled Diameter-Selective Dispersion of Semiconducting Single-Walled Carbon Nanotubes. *Chemistry of Materials* **2011,** *23*, 2237-2249.
[8] Stürzl, N.; Hennrich, F.; Lebedkin, S.; Kappes, M. M., Near Monochiral Single-Walled Carbon Nanotube Dispersions in Organic Solvents. *The Journal of Physical Chemistry C* **2009,** *113*, 14628-14632.
[9] Nish, A.; Hwang, J. Y.; Doig, J.; Nicholas, R. J., Highly selective dispersion of singlewalled carbon nanotubes using aromatic polymers. *Nature Nanotechnology* **2007,** *2*, 640-646.
[10] Hwang, J.-Y.; Nish, A.; Doig, J.; Douven, S.; Chen, C.-W.; Chen, L.-C.; Nicholas, R. J., Polymer Structure and Solvent Effects on the Selective Dispersion of Single-Walled Carbon Nanotubes. *Journal of the American Chemical Society* **2008,** *130*, 3543-3553.
[11] Chen, F.; Wang, B.; Chen, Y.; Li, L.-J., Toward the Extraction of Single Species of Single-Walled Carbon Nanotubes Using Fluorene-Based Polymers. *Nano Letters* **2007,** *7*, 3013-3017.
[12] Keogh, S. M.; Hedderman, T. G.; Gregan, E.; Farrell, G.; Chambers, G.; Byrne, H. J., Spectroscopic Analysis of Single-Walled Carbon Nanotubes and Semiconjugated Polymer Composites. *The Journal of Physical Chemistry B* **2004,** *108*, 6233-6241.
[13] Keogh, S. M.; Hedderman, T. G.; Lynch, P.; Farrell, G. F.; Byrne, H. J., Bundling and Diameter Selectivity in HiPco SWNTs Poly(p-phenylene vinylene-co-2,5-dioctyloxy-m-phenylene vinylene) Composites. *The Journal of Physical Chemistry B* **2006,** *110*, 19369-19374.
[14] Chen, J.; Liu, H.; Weimer, W. A.; Halls, M. D.; Waldeck, D. H.; Walker, G. C., Noncovalent Engineering of Carbon Nanotube Surfaces by Rigid, Functional Conjugated Polymers. *Journal of the American Chemical Society* **2002,** *124*, 9034-9035.
[15] Rice, N. A.; Soper, K.; Zhou, N.; Merschrod, E.; Zhao, Y., Dispersing as-prepared single-walled carbon nanotube powders with linear conjugated polymers. *Chemical Communications* **2006**, 4937-4939.
[16] Lemasson, F. A.; Strunk, T.; Gerstel, P.; Hennrich, F.; Lebedkin, S.; Barner-Kowollik, C.; Wenzel, W.; Kappes, M. M.; Mayor, M., Selective Dispersion of Single-Walled Carbon Nanotubes with Specific Chiral Indices by Poly(N-decyl-2,7-carbazole). *Journal of the American Chemical Society* **2011,** *133*, 652-655.
[17] Stuparu, A.; Stroh, C.; Hennrich, F.; Kappes, M. M., Dispersion of single walled carbon nanotubes using poly(3-dodecylthiophene-2,5-diyl). *physica status solidi (b)* **2010,** *247*, 2653-2655.
[18] Izard, N.; Kazaoui, S.; Hata, K.; Okazaki, T.; Saito, T.; Iijima, S.; Minami, N., Semiconductor-enriched single wall carbon nanotube networks applied to field effect transistors. *Applied Physics Letters* **2008,** *92*, 243112.
[19] Cheng, F.; Imin, P.; Maunders, C.; Botton, G.; Adronov, A., Soluble, Discrete Supramolecular Complexes of Single-Walled Carbon Nanotubes with Fluorene-Based Conjugated Polymers. *Macromolecules* **2008,** *41*, 2304-2308.
[20] Guo, X. G.; Kim, F. S.; Jenekhe, S. A.; Watson, M. D., Phthalimide-Based Polymers for High Performance Organic Thin-Film Transistors. *Journal of the American Chemical Society* **2009,** *131*, 7206-7207.
[21] Qian, G.; Qi, J.; Davey, J. A.; Wright, J. S.; Wang, Z. Y., Family of Diazapentalene Chromophores and Narrow-Band-Gap Polymers: Synthesis, Halochromism, Halofluorism, and Visible-Near Infrared Photodetectivity. *Chemistry of Materials* **2012,** *24*, 2364-2372.
[22] Song, S.; Park, S.; Kwon, S.; Lee, B. H.; Kim, J. A.; Park, S. H.; Jin, Y.; Lee, J.; Kim, I.; Lee, K.; Suh, H., Synthesis and characterization of phenathrothiadiazole-based conjugated polymer for photovoltaic device. *Synthetic Metals* **2012,** *162*, 1936-1943.
[23] Ponder, J. W. *TINKER*, 4.1; Washington University School of Medicine: Saint Louis, MO, **2003**.